Smooth inversion of Mt. Bulga data, with Rayfract® free trial version 3.22 :

Download our free trial and install it under Windows XP/Windows 2000/Windows Vista or Windows 7.

Start up Rayfract® trial 3.22 via desktop icon. Select *File|New Profile…* . Set *File name* to `BULGATRL` and click *Save button*. Specify *Station spacing* of 5 m in *Header|Profile* (Fig. 1).

Unzip archive mtbulga.zip in directory \RAY32\BULGATRL\INPUT.

Select *File|Import Data…* (Fig. 2) and specify *Import data type* `Interpex GREMIX .GRM`. Click *button Select* and select file MTBULGA.GRM in \RAY32\BULGATRL\INPUT.

Click *button Import shots*. Click *button Read* 9 times to import all 9 shots specified in MTBULGA.GRM. Do not edit any header fields.

Select *Refractor|Shot breaks*. Press ALT+P. Set *Maximum time* to 150 msecs. Hit ENTER key to redisplay traveltime curves. Select *Mapping|Color picked traveltime curves*. Browse curves with F7/F8 (Fig. 4).

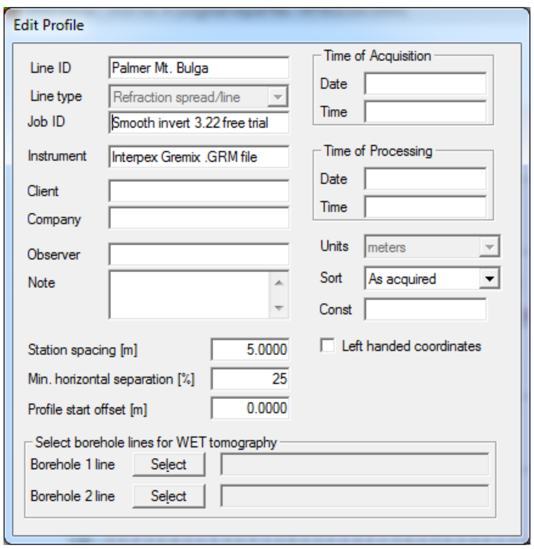

Fig. 1 : *Header|Profile*, edit profile header data

To invert the synthetic traveltime data with our *Smooth inversion* method :

- check *Smooth invert|Smooth inversion Settings|Wide smoothing filter for 1D initial velocity profile*
- run *Smooth invert|WET with 1D-gradient initial model*
- read *Shot point spacing is too wide warning prompt* (Fig. 3), recommending to position a shot at every 6th receiver instead of every 12th . Click *Yes button* to continue with Smooth inversion.
- confirm prompts to obtain Fig. 5, 6 and 7.

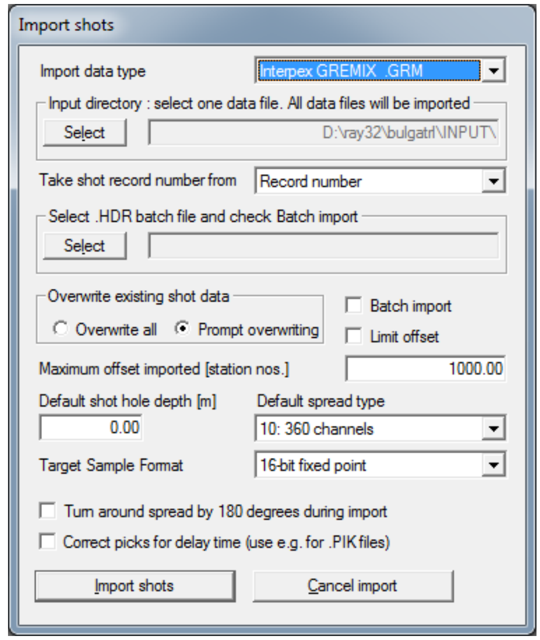

Fig. 2 : *File|Import Data…* dialog

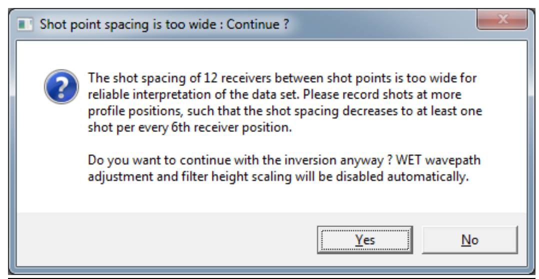

Fig. 3 : *Shot point spacing is too wide* warning prompt. Continue at your own risk.

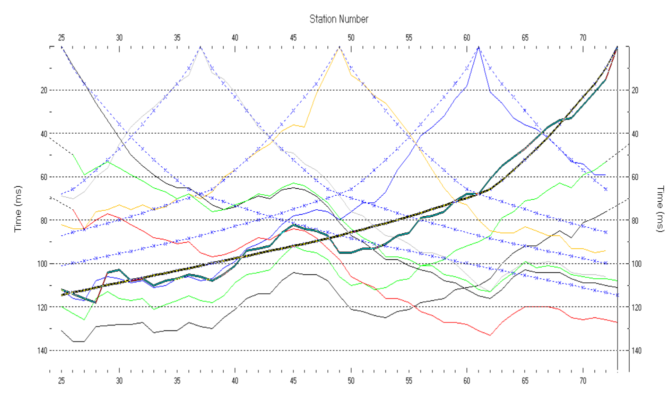

Fig. 4 : *Refractor|Shot breaks* display. Browse traveltime curves with F7/F8. Solid colored curves are picked times, dashed blue curves are modeled times, for starting model shown in Fig. 5 . RMS error is 7.1%.

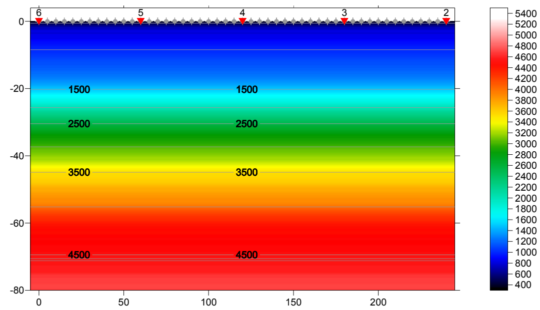

Fig. 5 : 1D starting model obtained with Smooth inversion, with default settings. RMS error is 7.1%. Horizontal/vertical axis in meters, color coding shows velocity in m/s.

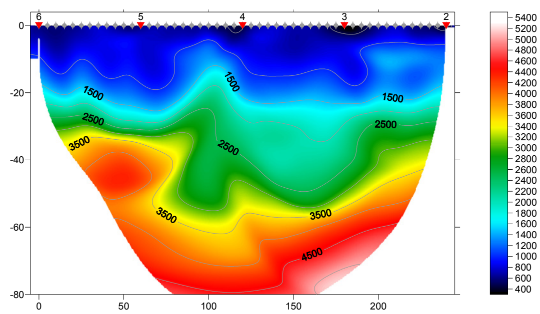

Fig. 6 : Velocity tomogram with Smooth inversion, 20 WET iterations, default settings, wavepath width 5.5%. RMS error is 2%. Starting model is Fig. 5.

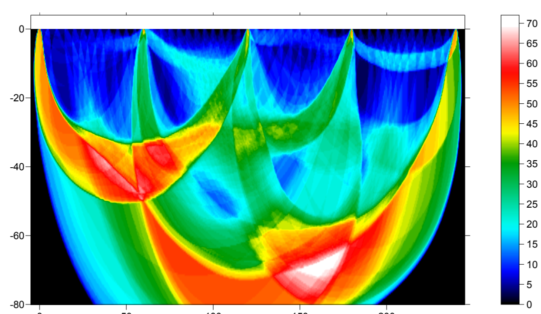

Fig. 7 : WET wavepath coverage obtained with Fig. 6. Color coding shows number of wavepaths per pixel / coverage of subsurface with first break energy.

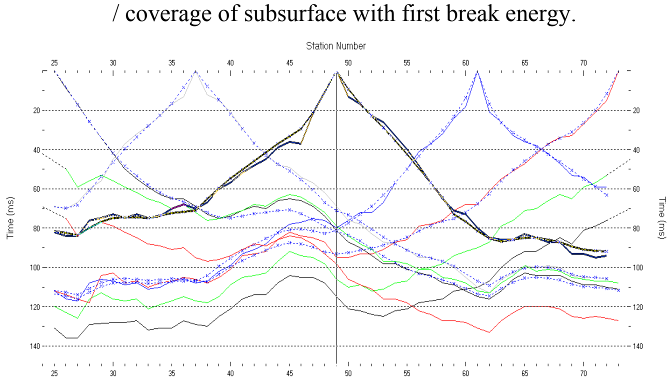

Fig. 8 : *Refractor|Shot breaks*, fit between picked (colored solid curves) and modeled (dashed blue curves) after 20 WET iterations. RMS error is 2%.

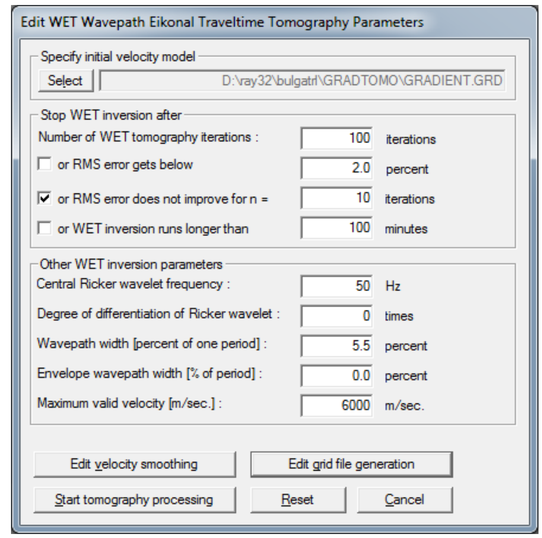

Fig. 9 : *WET Tomo|Interactive WET tomography…*

The following steps are not possible with the trial :

- select *WET Tomo|Interactive WET tomography*
- make sure *initial velocity model* is set to `\RAY32\BULGATRL\GRADTOMO\GRADIENT.GRD`
- change *Number of WET tomography iterations* from default 20 to new 100 (Fig. 9)
- edit other settings in *Stop WET inversion after frame* as shown in Fig. 9
- click *Edit grid file generation button*, and change *Store each nth iteration only* to 20
- click buttons *Accept parameters* and *Start tomography processing*. Obtain Fig. 10 and 11.

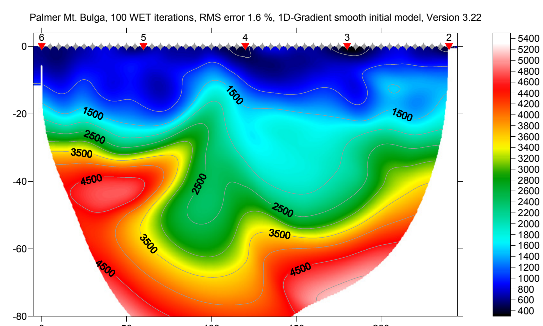

Fig. 10 : 100 WET iterations, wavepath width 5.5%. RMS error is 1.6%, starting model is Fig. 5.

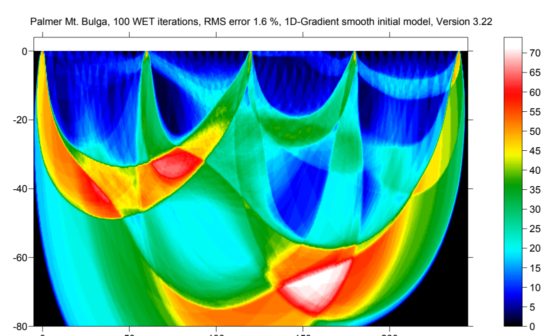

Fig. 11 : WET wavepath coverage shown with Fig. 10.

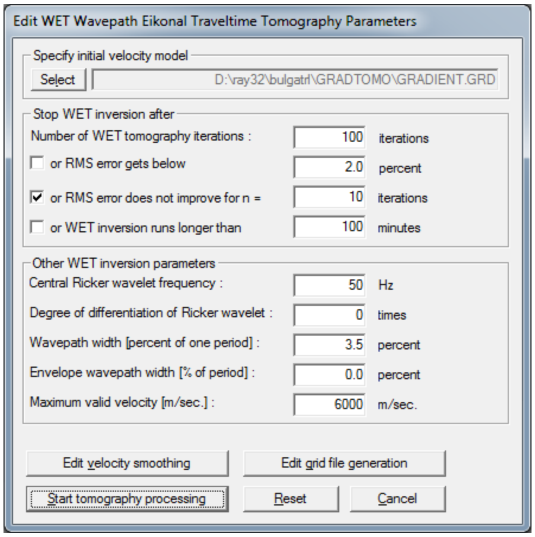

Fig. 12 : *WET Tomo|Interactive WET tomography…* , decrease *wavepath width* from default 5.5% to 3.5%

Next we decrease WET wavepath width (Fig 12) :

- select *WET Tomo|Interactive WET tomography*
- change *Wavepath width* from default 5.5% to new 3.5%
- click buttons *Accept parameters* and *Start tomography processing.* Obtain Fig. 13 and 14.

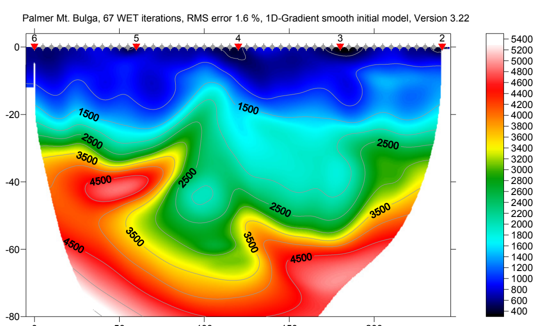

Fig. 13 : 67 WET iterations, wavepath width 3.5%. RMS error is 1.6%, starting model is Fig. 5.

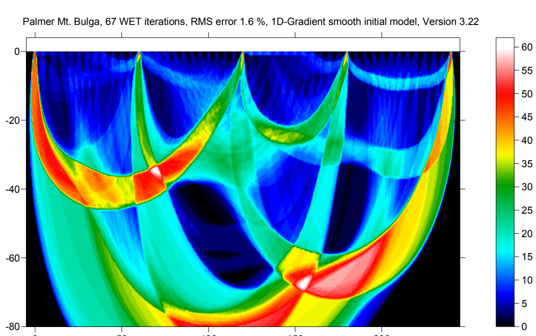

Fig. 14 : WET wavepath coverage shown with Fig. 13.

Next we increase WET wavepath width (Fig 15) :

- select *WET Tomo|Interactive WET tomography*

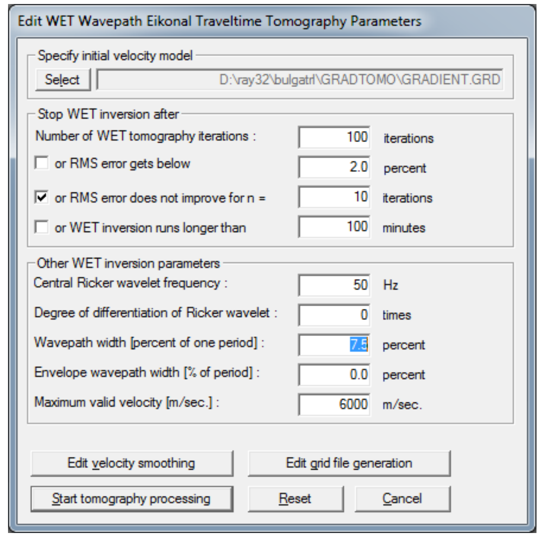

Fig. 15 : *WET Tomo|Interactive WET tomography…* , increase *wavepath width* from default 5.5% to 7.5%

- change *Wavepath width* from 3.5% to new 7.5%
- click buttons *Accept parameters* and *Start tomography processing.* Obtain Fig. 16 and 17.

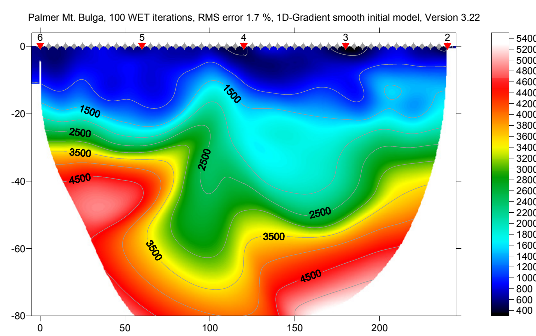

Fig. 16 : 100 WET iterations, wavepath width 7.5%. RMS error is 1.7%, starting model is Fig. 5.

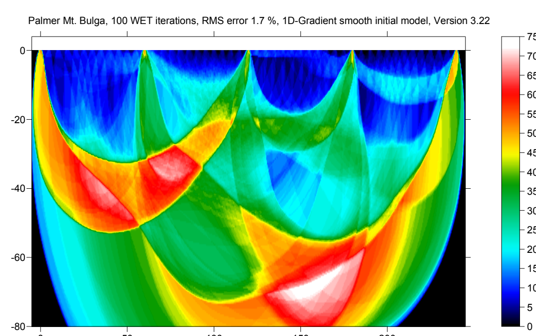

Fig. 17 : WET wavepath coverage shown with Fig. 16.

Next increase WET wavepath width to 15% (Fig. 18) :

- select *WET Tomo|Interactive WET tomography*
- change *Wavepath width* from 7.5% to new 15%
- click buttons *Accept parameters* and *Start tomography processing.* Obtain Fig. 19 and 20.

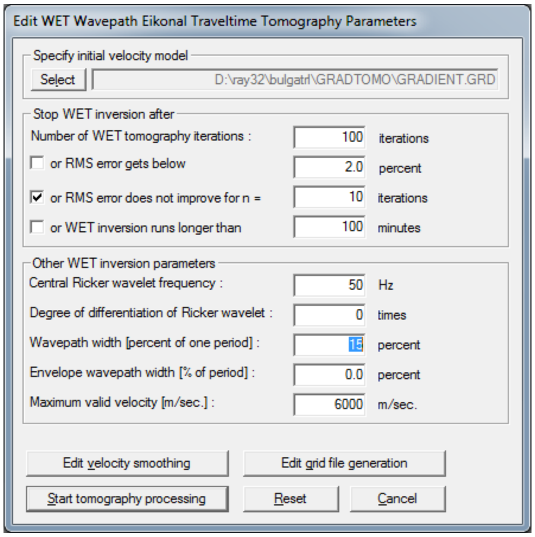

Fig. 18 : *WET Tomo|Interactive WET tomography…* , increase *wavepath width* from default 5.5% to 15%

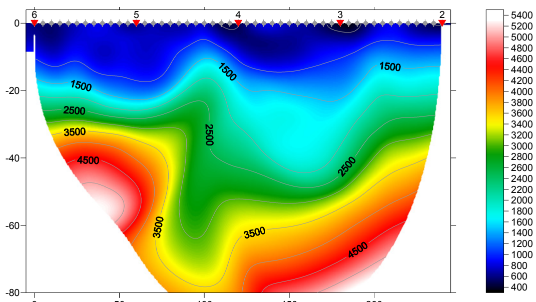

Fig. 19 : 100 WET iterations, wavepath width 15%. RMS error is 2%, starting model is Fig. 5.

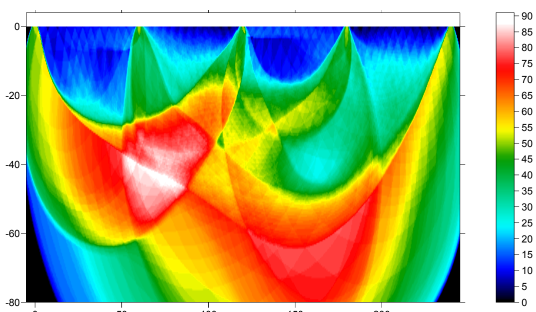

Fig. 20 : WET wavepath coverage shown with Fig. 19.

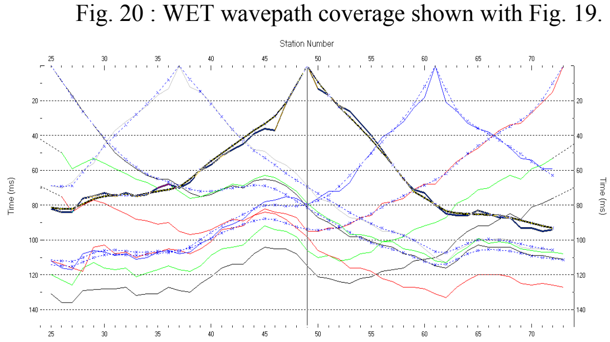

Fig. 21 : *Refractor|Shot breaks*, misfit after 100 WET iterations, wavepath width 15%. Compare Fig. 8.

Next we show WET output with same settings as in Fig. 18 and starting model Fig. 5, but with WET wavepath width increased to 30%, 50% and 100%.

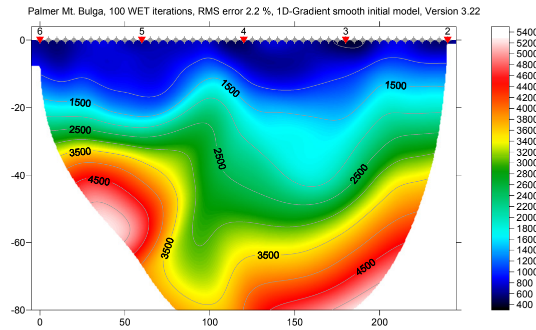

Fig. 22 : 100 WET iterations, wavepath width 30%. RMS error is 2.2%, starting model is Fig. 5.

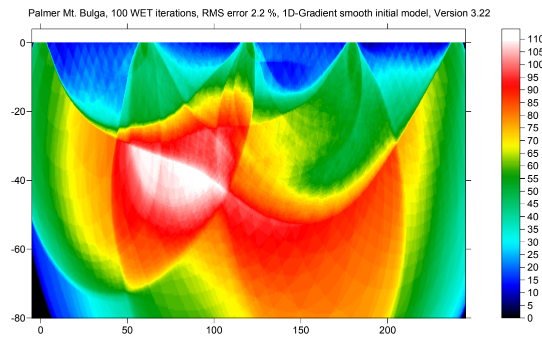

Fig. 23 : WET wavepath coverage shown with Fig. 22.

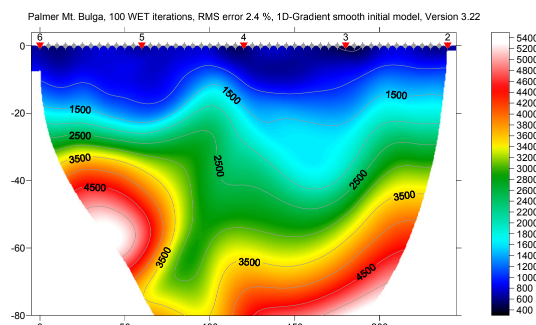

Fig. 24 : 100 WET iterations, wavepath width 50%. RMS error is 2.4%, starting model is Fig. 5.

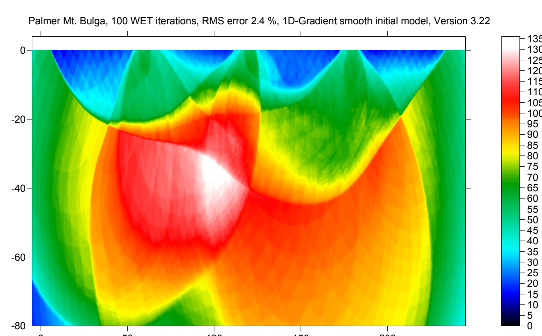

Fig. 25 : WET wavepath coverage shown with Fig. 24.

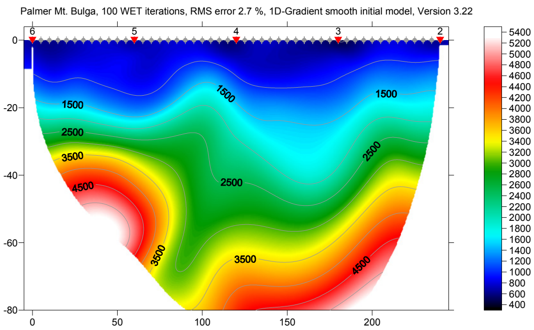

Fig. 26 : 100 WET iterations, wavepath width 100%. RMS error is 2.7%, starting model is Fig. 5.

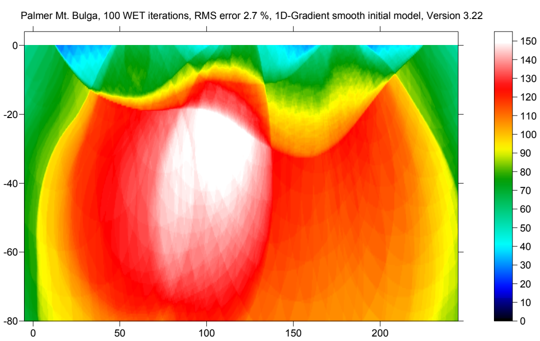

Fig. 27 : WET wavepath coverage shown with Fig. 26.

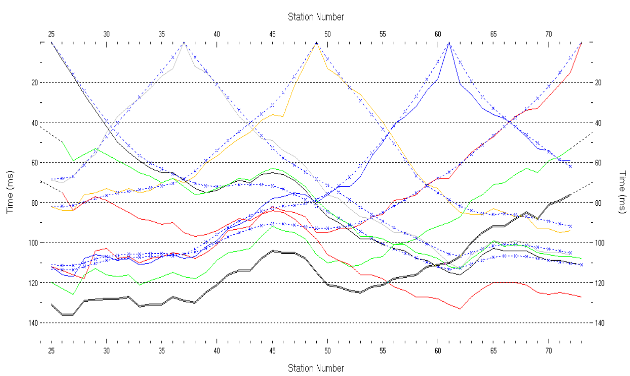

Fig. 28 : *Refractor|Shot breaks*, misfit after 100 WET iterations, wavepath width 100%. Compare Fig. 21.

We have shown how to explore the non-uniqueness of the model space, by varying WET wavepath width. Wider wavepath width results in less imaging artefacts, and smoother tomograms. This also decreases risk of unstable inversion and over-fitting to noisy or inconsistent (reciprocity, 2D assumption) traveltime data with bad picks.

The sub-vertical low-velocity fault zone remains visible throughout above tomogram series, while increasing wavepath width up to maximum possible value of 100%. So this fault zone is most certainly not an artefact of the processing, and is required to explain the traveltime data, even under minimum-structure assumption.

See our earlier interpretation mtbulga.pdf , showing layer-based Wavefront method and Smooth inversion with 999 iterations, using default wavepath width 5.5%. 100 iterations should be enough.

Run WET with 100 iterations and wide *wavepath width* of 50%. Then select tomogram grid `\RAY32\BULGATRL\GRADTOMO\VELOIT100.GRD` as starting model in Fig. 18, with *Select button*. Set *wavepath width* to smaller value e.g. 10% and do another 100 WET iterations. This gives a good image at bottom of tomogram due to wide wavepath width during 1st WET run, and also a good traveltime fit at near-offset channels due to more narrow width during 2nd WET run.

For inversion of synthetic traveltime data sets generated for known models, see tutorial thrust12, thrust, jenny10, epikinv, broadepi, fig9inv and SAGEEP11.pdf .

For more information on and instructions regarding our Smooth inversion method, see our short course notes SAGEEP10.pdf .

The best method to mitigate non-uniqueness of traveltime data interpretation is to **space shot points closely enough, at every 3rd receiver**. See SAGEEP10.pdf slide **Survey Design Requirements and Suggestions** on page 19 of 61**.** Also **pick traveltimes physically consistently**, regarding the reciprocity principle, to control non-uniqueness.

Smooth 2D inversion compared to conventional Wavefront interpretation of Palmer Mt. Bulga data set:

Siegfried Rohdewald, Dipl. Informatik-Ing. ETH, Vancouver Canada. E-mail: info@rayfract.com

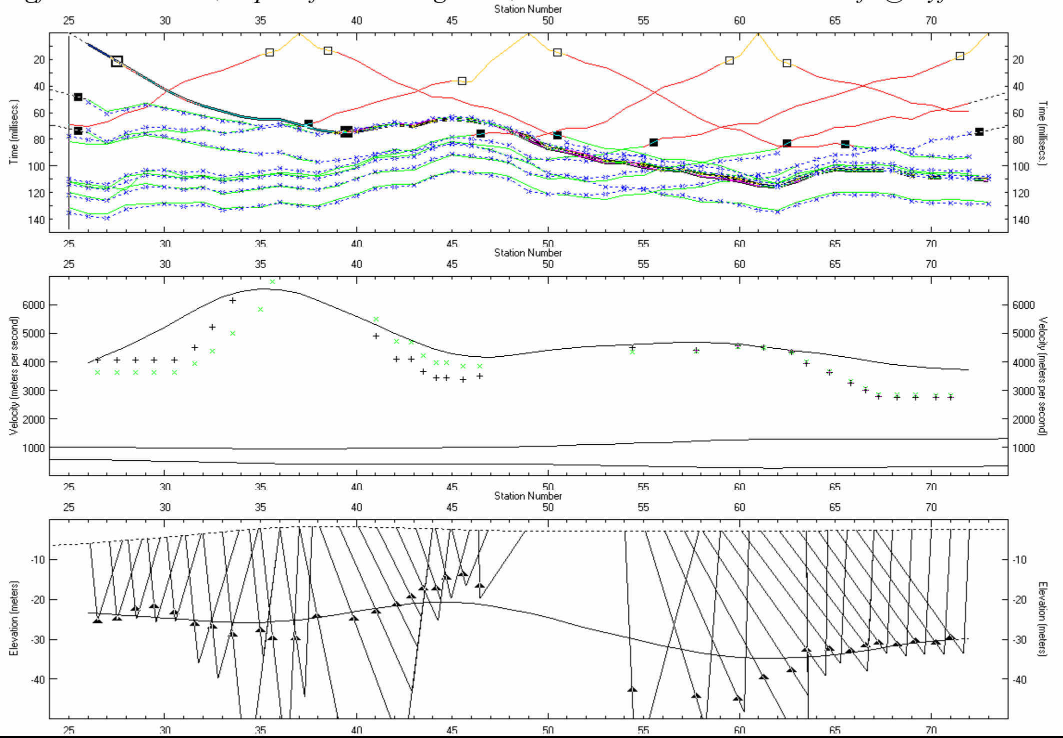

Fig. 1 Wavefront method interpretation (Jones and Jovanovich 1985), of Palmer Mt. Bulga data (Palmer 2003). Download from http://rayfract.com/tutorials/mtbulga.zip. Station spacing 5 meters. Top: map first breaks to refractors. Center: velocity, m/s. Bottom: refractor depth (m) below topography. Dashed line is weathering bottom. Triangles outline second (basement) refractor.

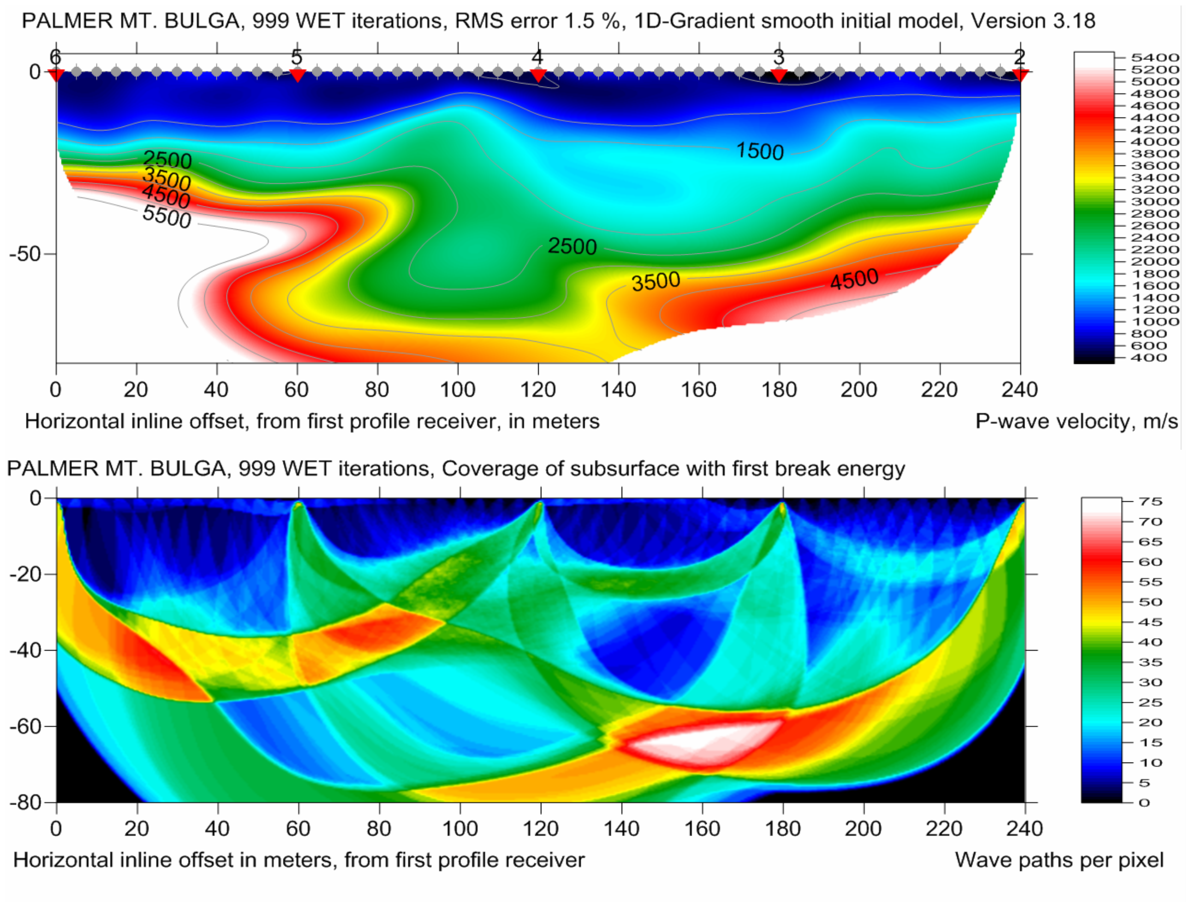

Fig. 2 Smooth 2D inversion version 3.18, 999 WET iterations (Schuster and Quintus-Bosz 1993), default parameters. Top: velocity. Bottom: wave path coverage . Note strong lateral velocity variation and velocity inversions in overburden. There are no laterally continuous refractors. Far-offset shots not regarded. We recommend to record shots with overlapping receiver spreads.

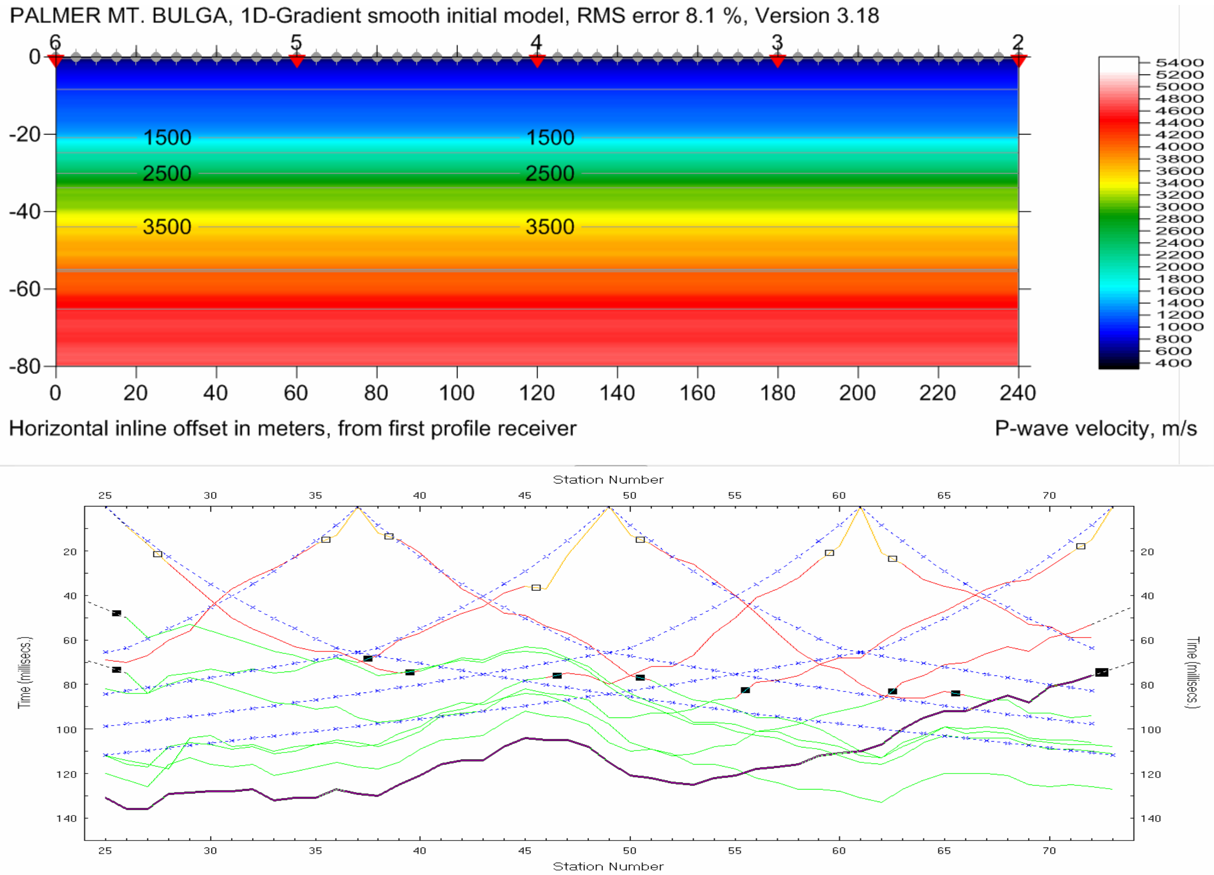

Fig. 3 Top: 1D-gradient initial model, determined with Delta-t-V method and default parameters. Bottom: fit between picked times (solid colored curves) and times modeled with Eikonal solver (dashed blue curves), for this 1D-gradient initial model. RMS error is 8.1 percent. Far-offset shots are not regarded.

Note the good correlation of basement depth, between the Smooth inversion (Fig. 2) and Wavefront interpretation (Fig. 1). For my Smooth inversion interpretation, I assume that the 2,500 m/s velocity contour represents the basement top. Below inline offset 0 meters to 80 meters, both methods show a basement depth of 25 to 30 meters. Also, both methods show a maximum basement depth of 45 to 50 meters, below inline offset 150 meters to 175 meters. Above shot spacing of 12 receivers is too wide for reliable Smooth inversion. We recommend an average shot spacing of 3 receivers or closer, see http://rayfract.com/tutorials/fig9inv.pdf and http://rayfract.com/SAGEEP10.pdf . Palmer (2003) uses the term "main refractor", with the same meaning as my usage of "basement". Smooth inversion does not regard far-offset shots positioned outside profile. Since four out of nine shots in this data set are far-offset shots, this may contribute to difference between Smooth inversion and GRM interpretation. We recommend overlapping receiver spreads. See http://rayfract.com/help/overlap.pdf .

In (Palmer 2003, Fig. 1) Dr. Palmer states that the line crosses a known major shear zone. His final interpretation (Palmer 2003, Fig. 4) shows a subvertical zone. I show a zone dipping to the left (Fig. 2). At a depth of 20 meters, we both agree on a zone centered at inline offset of about 150 meters. Obviously Dr. Palmer has decreased WET smoothing and wavepath width, and only run a few iterations, in (Palmer 2003, Fig. 3 to 5). Such poor settings effectively cripple WET, and resulting output will be very similar to the initial model. Default WET smoothing and wavepath width will give output with fewer artifacts (Fig. 2). We recommend to run at least 50 to 100 WET iterations, instead of the default 20 iterations. When I proposed to Dr. Palmer to drill a hole at the center of the profile, he replied that he did not remember the exact location of the line, and there would be a lot of trees now. For a synthetic fault model study showing imaging of a similar dipping low-velocity anomaly see http://rayfract.com/tutorials/thrust.pdf .

Resolution of WET and seismic refraction tomography in general decreases with increasing depth. See e.g. http://rayfract.com/tutorials/thrust.pdf , D.J. White 1989 Two-Dimensional Seismic Refraction Tomography and J.G. Hagedoorn 1959 The Plus-Minus method of interpreting Seismic Refraction Sections Fig. 1 .

Whiteley and Leung (2006) compare their VIRT interactive ray tracing interpretation to my Smooth inversion output, for above data set. They obtain similar depths and velocities, that compare well with the extensive drilling, carried out earlier, to explore the Mt. Bulga ore body.

For a systematic evaluation of our Smooth inversion method, see Sheehan et al. (2005a). Smooth inversion is based on a 1D gradient initial model (Fig. 3) as determined with our Delta-t-V inversion (Gebrande and Miller 1985, Winkelmann 1998), to avoid velocity artefacts. This initial model is refined iteratively with true 2D Wavepath Eikonal Traveltime inversion WET (Schuster and Quintus-Bosz 1993). While the Delta-t-V method is similar to the tau-*p* method (Diebold and Stoffa 1981; Barton and Barker 2003), Delta-t-V automatically detects and models velocity inversions (Winkelmann 1998: XTV method). While it may not always be possible to image velocity inversions, Smooth inversion output correctly shows the averaged velocity trends (Sheehan et al., 2005b). Delta-t-V detects and models layer internal constant velocity gradients (linear increase of velocity with depth). Velocity may jump discontinuously at layer boundaries.

In our experience, WET true 2D tomography processing requires a simple initial model which shows a good fit between picked and modeled traveltimes (Fig. 3). Otherwise WET may get stuck in a local minimum of the traveltime misfit function (Schuster and Quintus-Bosz 1993, eqn. (1)), especially if the initial model and grid are too shallow. Our WET implementation will not increase the depth of a too shallow initial grid.

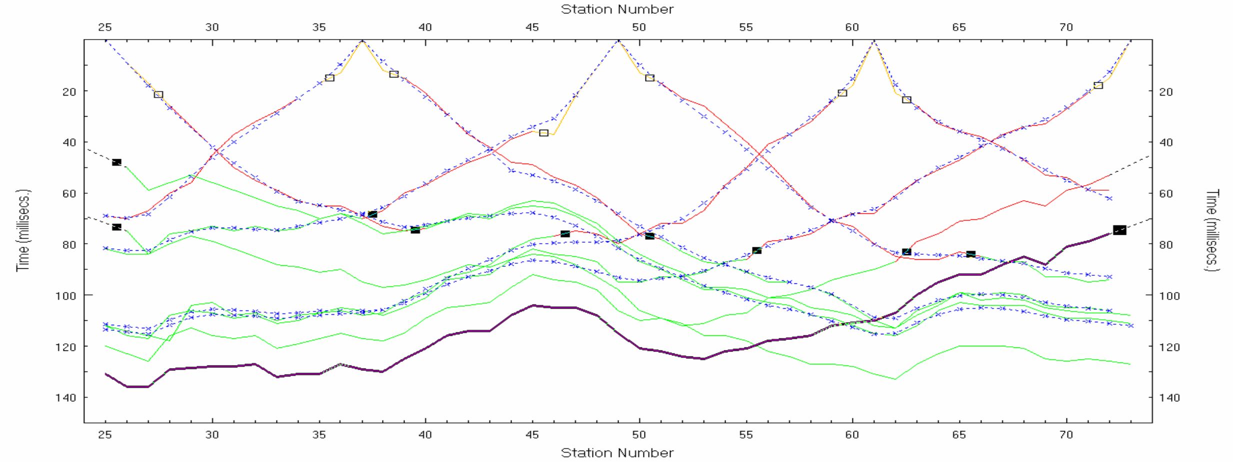

Fig. 4 Fit between picked traveltimes (solid colored curves) and modeled times (dashed blue curves), after 999 WET iterations. The RMS error is 1.5 msec. Hollow squares separate direct wave (yellow) from 1st refractor (red). Filled squares separate 1st from 2nd refractor (green). Assignment of traces to refractors is not required for Smooth inversion and WET.

As shown by Sheehan et al. (2005a, 2005b), Smooth inversion and Seismic Refraction Tomography in general vertically blur the basement top. But conventional methods such as Wavefront (Jones and Jovanovich 1981) and Generalized Reciprocal Method GRM (Palmer 1981) are based on the often unrealistic assumption that the subsurface can be modeled with a few laterally continuous layers with no vertical velocity gradient. Such layers are mathematically idealized refractors, with constant layer-internal velocity below constant inline offset. These conventional methods suppress a common basement-internal, positive velocity gradient (Fig. 3 and 4, highlighted shot) and project the average basement-internal velocities to the basement top. So these methods typically give a too high estimate, for the seismic velocity at the top of the basement.

Also, faults, velocity inversions, local velocity anomalies, pinchouts, outcrops and vertical velocity gradients within layers often make the interactive assignment of first breaks to laterally continuous idealized refractors difficult and ambiguous. See Fig. 3 and 4, e.g. shots located at station number 49 and higher. Delta-t-V does not require the user to carry out such a subjective assignment, while conventional methods such as GRM and Wavefront do. Mechanical and chemical weathering cause the rock quality and seismic velocity to decrease the closer the rock or sediment unit is to the surface. In other words, rock quality and seismic velocity tend to increase with increasing burial depth. See e.g. (B. Murck 2001), chapter 6 (Weathering and Erosion) : joints, exfoliation and frost wedging.

Leung (1995; 2003) and Sjögren (2000) describe the non-uniqueness inherent in the determination of the optimum XY value, as required for the GRM (Palmer 1981). GRM assumes that the XY value is constant for the whole profile. In case of strong lateral velocity variation, a too short estimated XY value may then result in a too low derived overburden velocity, and too shallow imaged basement. Our Wavefront method automatically determines a laterally varying XY receiver separation. See Jones and Jovanovich (1985), Brueckl (1987) and Ali Ak (1990). Wavefront considers local emerging wavefront angles. A critically refracted ray is represented by first break and emergence angle at a receiver. Each reverse ray is combined with a matching forward ray, such that both rays surface from an approximated common refractor location.

We thank Dr. Palmer for making available this interesting data set. You can download the original data from http://rayfract.com/tutorials/mtbulga.zip .

REFERENCES

Ali Ak M. 1990. An analytical raypath approach to the refraction wavefront method. Geophysical Prospecting, volume 38, pp. 971-982.

Barton P. and Barker N. 2003. Velocity imaging by tau-*p* transformation of refracted seismic traveltimes. Geophysical Prospecting, volume 51, pp. 195-203.

Brueckl E. 1987. The Interpretation of Traveltime Fields in Refraction Seismology. Geophysical Prospecting, volume 35, pp. 973-992.

Diebold J.B. and Stoffa P.L. 1981. The traveltime equation, tau-p mapping, and inversion of common midpoint data. Geophysics, volume 46, pp. 238-254.

Gebrande H. and Miller H. 1985. Refraktionsseismik (in German). In: F. Bender (Editor), Angewandte Geowissenschaften II. Ferdinand Enke, Stuttgart; pp. 226-260. ISBN 3-432-91021-5.

Jones G.M. and Jovanovich D.B. 1985. A ray inversion method for refraction analysis. Geophysics, volume 50, pp. 1701-1720.

Leung T.M. 1995. Examination of the optimum XY value by ray tracing. Geophysics, volume 60, pp. 1151-1156.

Leung T. M. 2003. Controls of traveltime data and problems of the generalized reciprocal method. Geophysics, volume 68, pp. 1626-1632.

Murck B. 2001. Geology. A Self-Teaching Guide. John Wiley & Sons, Inc., New York. ISBN 0-471-38590-5.

Palmer D. 1981. An Introduction to the generalized reciprocal method of seismic refraction interpretation. Geophysics, volume 46, pp. 1508-1518.

Palmer D. 2003. Application of amplitudes in shallow seismic refraction inversion: 16th Geophysical Conference and Exhibition, Australian Society of Exploration Geophysicists.

Schuster G.T. and Quintus-Bosz A. 1993. Wavepath eikonal traveltime inversion: Theory. Geophysics, volume 58, pp. 1314-1323.

Sheehan J.R., Doll W.E. and Mandell W.A. 2005a. An Evaluation of Methods and Available Software for Seismic Refraction Tomography. Journal of Environmental and Engineering Geophysics, volume 10, pp. 21-34. ISSN 1083-1363, Environmental and Engineering Geophysical Society. JEEG March 2005 issue.

Sheehan J.R., Doll W.E., Watson D.B and Mandell W.A. 2005b. Application of Seismic Refraction Tomography to Karst Cavities. U.S. Geological Survey Scientific Investigations Report 2005-5160.

Sjögren B. 2000. A brief study of applications of the generalized reciprocal method and of some limitations of the method. Geophysical Prospecting, volume 48, pp. 815-834

Whiteley B. and Leung T.M. 2006. Mt. Bulga Revisited. http://rayfract.com/pub/Mt_Bulga_Revisited.pdf.

Winkelmann R.A. 1998. Entwicklung und Anwendung eines Wellenfeldverfahrens zur Auswertung von CMP-sortierten Refraktionseinsaetzen. Akademischer Verlag Muenchen, Munich. ISBN 3-932965-04-3.